

# Microstructural Analysis and Mechanical Behaviour of Epoxy Composites With a Very High Nanofiller Content Synthetized by High Energy Ball Milling

UDC:678.7:620.17

Original scientific paper

<https://doi.org/10.46793/aeletters.2026.11.2.3>S. Grairia<sup>1\*</sup>, R. Slimani<sup>1</sup>, A. Maanser<sup>2</sup>, A. Saoudi<sup>3</sup>, A. Ballah<sup>1</sup>

<sup>1</sup>Research Laboratory in Energy and Materials "RLEM", Faculty of Science and Technology, University of Tamanghasset, 11000 Tamanghasset, Algeria

<sup>2</sup>Department of Architecture, Larbi Ben Mhidi University, 4000 Oum El-Bouaghi, Algeria

<sup>3</sup>Scientific and Technical Research Center in Physico-Chemical Analyses (STRCPA), Industrial zone BP 384, Bou-Ismaïl, 42000 Tipaza, Algeria

## Abstract:

This study examines the addition of silica sand nanoparticles at 12 wt.%, 22 wt.%, 32 wt.%, 42 wt.%, 52 wt.%, and 62 wt.% into epoxy resin matrices (DGEBA, Medapoxy HR EA, and Medapoxy HR EB) to enhance their physical, mechanical, and microstructural properties. In research, Silica was successfully incorporated up to 42 wt.%, exceeding the typical 25 wt.% inorganic threshold. This incorporation significantly boosts the compressive, flexural, and tensile strengths of the nanocomposites to 113.685 MPa, 49.723 MPa, and 33.452 MPa, respectively, showing increases of 57.49%, 40.33%, and 37.31% over pure epoxy. The optimal silica content for maximizing mechanical properties lies between 32 wt.% and 42 wt.%. Scanning electron microscopy (SEM) reveals that pure epoxy has a smooth and brittle fracture surface, whereas epoxy/SiO<sub>2</sub> composites exhibit cohesive deformations and fractures due to the silica. However, silica content above 42 wt.% leads to nanoparticle agglomeration, which reduces performance. The study concludes that silica nanoparticles improve the mechanical properties of epoxy resin, making the nanocomposites more economical, durable, and suitable for various industrial and domestic applications. These findings support the development of high-performance materials from abundant natural byproducts.

## ARTICLE HISTORY

Received: 1 October 2025

Revised: 4 May 2026

Accepted: 29 May 2026

Published: 29 June 2026

## KEYWORDS

Natural Silica sand, Epoxy resin, Nanocomposites, High energy ball milling, Mechanical properties, Microstructure, Fracture surface

## 1. INTRODUCTION

Epoxy resins are versatile thermosetting polymers with high performance and ease of processing, typically containing at least two epoxy groups per molecule. Their high reactivity makes them suitable for various mechanical applications, owing to their excellent adhesive properties, rigidity, dimensional stability, chemical resistance, and high fluidity before curing [1-4]. However, epoxy resins, when made from highly cross-linked polymers, are often brittle and prone to low resistance to crack propagation [5].

Numerous studies [6] have focused on improving the mechanical properties of pure epoxy resin, particularly by incorporating fillers such as glass particles, ceramics, silicates, and rubbers [7-9]. Other research [10,11] has examined the impact of particle size, degree of dispersion, and filler content on the resulting composite's mechanical strength. The mechanical properties of particulate composites can vary considerably depending on factors such as chemical composition, particle shape and size, the particle-matrix interface, particle distribution, and manufacturing conditions (such as curing temperature and resin-to-hardener ratio) [12,13].

\*CONTACT: S. Grairia, e-mail: [said.grairia@univ-tam.dz](mailto:said.grairia@univ-tam.dz)

In contrast to prior studies, which examined many fillers for their individual effects on epoxy resins, this paper introduces a novel approach by incorporating silica-rich sand powder to form a particulate composite. The inclusion of this naturally sourced sand powder is advantageous due to its strong adsorption capabilities when combined with epoxy resin [14]. Unlike previous research, in which nanoparticles are typically produced synthetically at a higher cost, this study presents a cost-effective ball-milling technique to produce nanosized mineral fillers from natural siliceous sand. This approach addresses the need for a more sustainable and economically viable method of improving epoxy composites, especially for applications requiring low-cost production.

Furthermore, this research uniquely explores the effects of varying filler content (12 wt.%, 22 wt.%, 32 wt.%, 42 wt.%, 52 wt.%, and 62 wt.%) on the physical, mechanical, and microstructural properties of the epoxy composite. Particular focus is placed on the high SiO<sub>2</sub> content and low epoxy resin content, resulting in an "economical" composite with reduced resin usage. This is an important development for industries aiming to reduce material costs without sacrificing performance.

The aim of this research is twofold: 1) to produce nano-sized mineral fillers from natural siliceous sand using a cost-effective ball-milling technique, and 2) to investigate the influence of these nanofillers, used as a partial substitute for epoxy resin, on the physical, mechanical, and fracture surface microstructure of the composite. This dual-focus approach offers new insights into optimizing epoxy composites for cost-effective and high-performance applications.

## **2. MATERIALS AND METHODS**

### **2.1. Preparation of Silica Sand Nanoparticle**

High-energy ball milling of natural silica sand can yield anisotropic silica nanoparticles with controlled structures [15,16]. An optimal grinding time of 48 h converts micrometric sand into truly nanometric particles (~76 nm) while preserving quartz crystallinity (SiO<sub>2</sub>) and high purity.

This duration balances effective size reduction with minimal agglomeration, phase change, or contamination, remaining practical and cost-effective for large-scale composites.

Silica sand from Tebessa (Algeria) was washed, dried at 105°C, dry ball-milled with zirconia balls, and sieved (Sieve Shaker/EFL2000) using a top-down approach. Particle size was measured by

Zetasizer Nano ZS (ZEN 3600, MALVERN), morphology by SEM, and composition by XRF at LMOPS/SUPELEC Metz (France) [17].

### **2.2. Specimen Preparation and Curing**

The polymer and hardener were used in a 100/60 ratio as recommended, with silica powder first dried at 105°C for 1 h, then weighed and mixed with MEDAPOXY HR EA (pre-polymer) for 3 min, followed by the addition of MEDAPOXY HR EB (curing agent) and another 3 min of mixing. The mixture was cast into molds coated with a debonding agent, demolded after 24 h, and allowed to cure at room temperature for up to 28 days before mechanical testing [18].

Processing, which accounts for about 50–60% of production costs, strongly affects microstructure and final properties, so improving particulate-reinforced epoxy composites is a major concern for industry and research [19]. Typical manufacturing routes aim to reduce resin viscosity and surface tension and enhance particle dispersion through mechanical shear mixing, ultrasound sonication, chemical and thermal methods, vacuum degassing, and nanoparticle reinforcement [20–22], as these combined techniques improve particle dispersion and, in turn, composite performance. Key limitations in processing particulate polymeric composites include controlling dispersion and homogeneity, avoiding agglomeration, and managing matrix-reinforcement interfacial effects.

Adding reinforcement changes most polymer properties (sometimes positively, sometimes negatively), and in this work, residual stresses were reduced by a simple manual mixing sequence where particles were first dispersed in the polymer and then in the hardener. Studies report that simple mechanical stirrers may not supply enough energy to generate adequate shear stress, leading to poor particle coverage by the epoxy matrix [23], while particle size, shape, aspect ratio, agglomeration tendency, and moisture absorption also affect mechanical behaviour [24].

Industrial-scale processes such as flow-through bins and pneumatic moulds improve properties by inducing disturbance and vibration, so that fine particles fill the voids between larger ones and increase packing density [25,26]. However, hand mixing was ultimately chosen here for its low cost, ease of use, flexibility in size and thickness, broad applicability, and reproducibility, as confirmed by a coefficient of variation below 20%, indicating variability lower than usually expected in manufacturing [27].

### 2.3. Specimen Dimensions and Testing Procedures

Mechanical tests in compression, uniaxial tension, and three-point bending were carried out on a Zwick/Rowell machine equipped with a 2.5 kN static load cell: for compressive tests, 5 cubic samples (40 mm x 40 mm x 40 mm) per mix were tested at 1.25 mm/min, in accordance with ASTM C349. For three-point bending tests, 5

parallelepipedic samples (4×4×16 cm) per mix were machined at a rate of 1 mm/min, in accordance with ASTM C 348-97. For tensile tests, 5 samples per mix were used, with dimensions of 105±2 mm long, 10±2 mm wide, and 4±2 mm thick, in accordance with ASTM D-638-91 (Type I). For density tests, samples are tested in accordance with ASTM D 792-08. A displacement-controlled machine was used for compression, three-point bending, and tensile tests, as shown in Fig. 1.

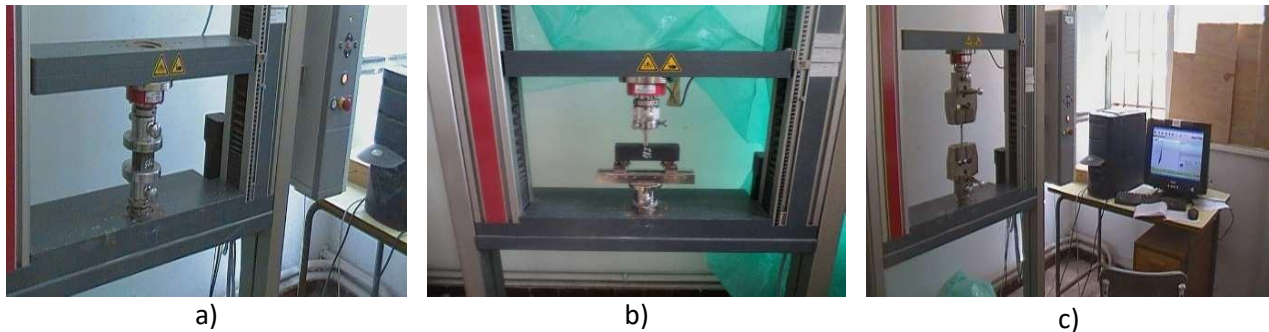


Fig. 1. Control machine for: (a) compression test, (b) three-point bending test and (c) tensile test

### 2.4. Characterization Methods

Pure epoxy, silica nanoparticles, and epoxy-silica nanoparticle hybrid samples with various silica contents were characterized using the techniques described below.

#### 2.4.1. Energy Dispersive X-Ray Analysis (EDAX)

EDAX microanalysis is an elemental analysis technique coupled with electron microscopy, based on the generation of characteristic X-rays that identify the elements present in the specimens. Our samples were analyzed by EDAX at the Laboratory for the Study of Microstructures and Mechanics of Materials, National School of Mines and Metallurgy, Annaba (Algeria).

#### 2.4.2. X-Ray Diffraction (XRD)

XRD analysis is used to determine the silica phase of the sand powder samples, which are scanned using an X-ray diffractometer at the Laboratory for the Study of Microstructures and Mechanics of Materials (LEM3), Metz, University of Lorraine (France).

#### 2.4.3. X-Ray-Fluorescence Spectroscopy (XRF)

The chemical composition of the Ground Natural Silica Sand GNSS, obtained by ball milling process, and of the hybrid nanocomposites was

analyzed using X-Ray Fluorescence spectroscopy (XRF) in the Analysis Laboratory LMOPS / SUPELEC Metz (France).

#### 2.4.4. Scanning Electron Microscopy (SEM)

The dispersion of silica nanoparticles and morphological studies were carried out by SEM available at the Material Laboratory of the National School of Arts and Crafts (NSAC), Paris-Tech, Lille (France), and the National School of Mines and Metallurgy, Annaba (Algeria). Nanocomposites are placed on an alumina plate and sputter-coated with a thin gold layer under vacuum to prevent the accumulation of static electric fields caused by electro-irradiation during imaging and to avoid charging before SEM observation.

### 2.5. Physical Measurements

The density of the epoxy-silica nanocomposites was measured at room temperature according to ASTM D792-20 using Archimedes' principle, with distilled water as the flotation fluid and cubic samples. An analytical balance (accuracy ± 1 mg) was used to weigh each sample in air and in water. Five specimens were measured for each system. The density of the samples  $\rho_s$  was calculated using the following expression according to ASTM D792-20 [28]:

$$\rho_s = \frac{w_{sa}}{w_{sa} - w_{sl}} \cdot \rho_l \quad (1)$$

where:  $w_{sa}$  - is its weight in air;  $w_{sl}$  - is its weight in a liquid;  $\rho_l$  - is the liquid's density (for distilled water,  $\rho_l = 1.0 \text{ g/cm}^3$ ).

## 2.6. Mechanical Measurements

All mechanical tests (traction, bending, and compression) were carried out in the Civil Engineering Department laboratory at Badji Mokhtar University of Annaba using a Zwick ZHU 2.5 universal testing machine (Fig. 1), and mechanical performance refers to strength in flexure, tension, and compression.

### 2.6.1. Compressive Testing

The compressive strength ( $\sigma_c$ ) of the nanocomposite specimens was measured according to ASTM C349 [29] using a Zwick ZHU 2.5 machine with a maximum load of 2.5 kN (Fig. 1a). Cubic specimens of 40 mm x 40 mm x 40 mm (Fig. 1a) were tested at a displacement rate of 1.25 mm/min, and a temperature of  $23 \pm 1^\circ\text{C}$ , and the reported ( $\sigma_c$ ) values are the averages of five specimens loaded until failure.

### 2.6.2. Flexure Testing

The flexural strength ( $\sigma_f$ ) of nanocomposite specimens was measured according to ASTM C 348- 97 using a Zwick ZHU 2.5 Universal Testing Machine with a maximum load capacity of 2.5 kN (Fig. 1b), following a three-point bending method with a support span of 100 mm, a crosshead speed of 1.0 mm/min, and a temperature of  $23 \pm 1^\circ\text{C}$ . Specimens measuring 40 mm x 40 mm x 160 mm (Fig. 1b) were tested, and the reported flexural strength ( $\sigma_f$ ) is the average of five specimens loaded to failure.

### 2.6.3. Tensile Testing

Tensile tests were carried out at room temperature ( $23 \pm 1^\circ\text{C}$ ) on dumbbell-shaped specimens (ASTM D- 638-91, Type I) machined by CNC from 4 mm thick moulded plates, using a Zwick ZHU 2.5 universal testing machine at a constant crosshead speed of 1 mm/min, in accordance with BS EN ISO 527:1996 (Fig. 1c). The dumbbell specimens had an overall length of 170 mm, with a narrow section 10 mm long and 4 mm wide (Fig. 1c), and the reported tensile strength values ( $\sigma_t$ )

are averages from five specimens loaded until failure.

## 3. RESULTS AND DISCUSSIONS

### 3.1. Morphology, Size and Distribution Analysis of Silica Sand Nanoparticles

Silica sand particles in the macro/micro-scale were reduced by high-energy milling (comminution by collisions) to nanoscale silica sand ( $\text{SiO}_2$ ) nanoparticles, with an initial size  $d < 630 \mu\text{m}$  (manufacturer/supplier) and final average size 76.34 nm as measured by Zeta-Sizer (Fig. 2, Table 1), thus qualifying them as  $\text{SiO}_2$  nanoparticles. SEM images (Fig. 3) show  $\text{SiO}_2$  nanoparticles with spherical and irregular shapes, forming agglomerates in which primary particles cluster or fuse at their faces, likely due to growth and 'sintering' during the ball-milling process, with a strong tendency to agglomerate induced by Van der Waals forces.

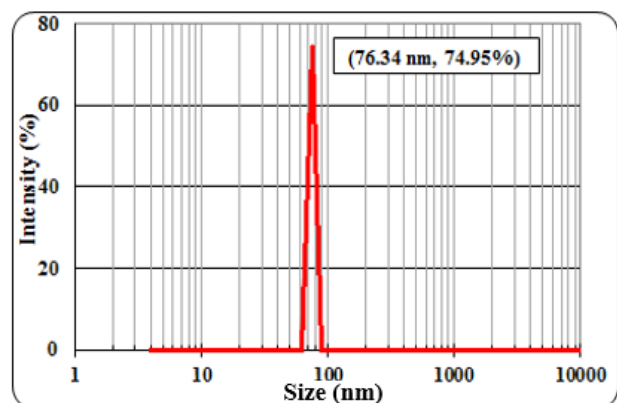


**Fig. 2.** PSA results of 48 hours of milled silica sand produced by Zeta-Sizer Nano Analyzer: Size and distribution of the silica sand nanoparticles (the average is 76.34 nm)

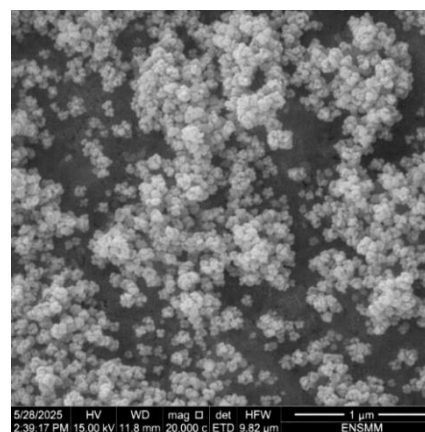


**Fig. 3.** SEM image of 48-hour ball-milled silica sand

The agglomerates exhibit morphologies ranging from chainlike (1-D) to heavily aggregated (3-D), and such soft agglomerates, held only by Van der Waals forces, are not considered a major problem and can even be beneficial for good thermal conduction [30].

**Table 1.** Size of milled natural silica sand

Sample type	Duration of grinding (h)	Particle size (Average)	Percentage (%) reduction in size
UMSS	-	< 630 μm	-
MNSS	48	76.34 nm	74.95

Note: **UMSS** - UnMilled Silica Sand, **MNSS** - Milled Nano Silica Sand.

### 3.2. Energy Dispersive X-Ray Analysis (EDAX)

Fig. 4 presents the EDAX spectrum of natural silica sand milled for 48 hours, showing mainly silicon (Si) and oxygen (O), with low percentages of aluminium (Al) and potassium (K), confirming SiO<sub>2</sub> and indicating that Al and K are natural sand constituents with no other contaminations detected after 48 hours of milling.

Because ball milling is performed under atmospheric conditions for extended periods, the EDAX results show oxygen atomic percentages approximately twice those of silicon, confirming the presence of silicon and oxygen in all samples.

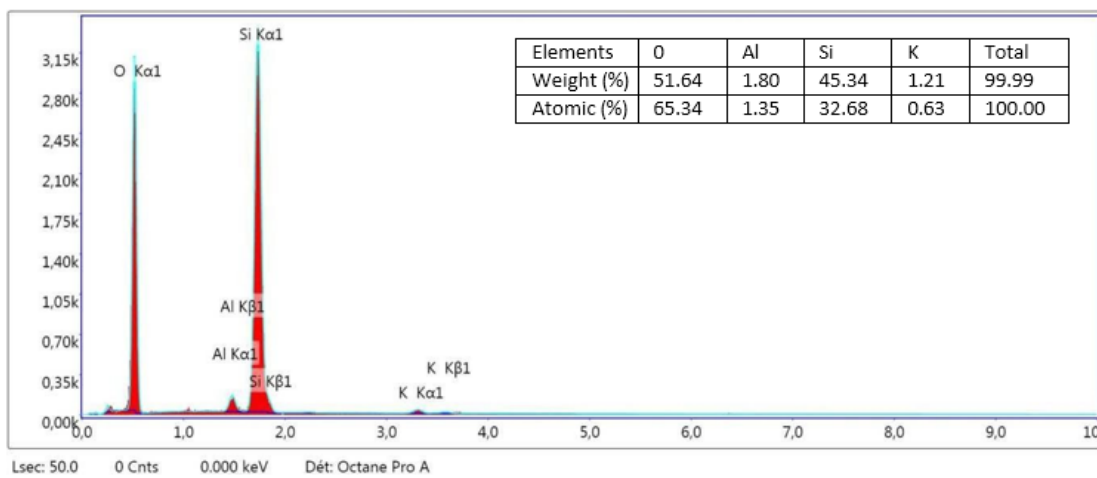


**Fig. 4.** EDAX Images (analysis) of 48 hours ball milled sand: EDAX spectrum (Energy Selection Spectroscopy) confirming the composition of the siliceous sand reinforcement

### 3.3. X-Ray Diffraction (XRD)

X-ray diffraction of SiO<sub>2</sub> nanopowder prepared from natural silica sand (quartz sand) milled for 48 hours showed peaks at orientations (100), (101), (110), (200), (112), (103), (203), (231)..., confirming that the milled powder is SiO<sub>2</sub> material. The XRD

pattern in Fig. 5 corresponds to quartz (SiO<sub>2</sub>) peaks reported in the Joint Committee on Powder Diffraction Standards (JCPDS) database and relevant literature [31], with a typical silicon dioxide peak and identification of quartz (SiO<sub>2</sub>) as the main crystalline phase in the filler.

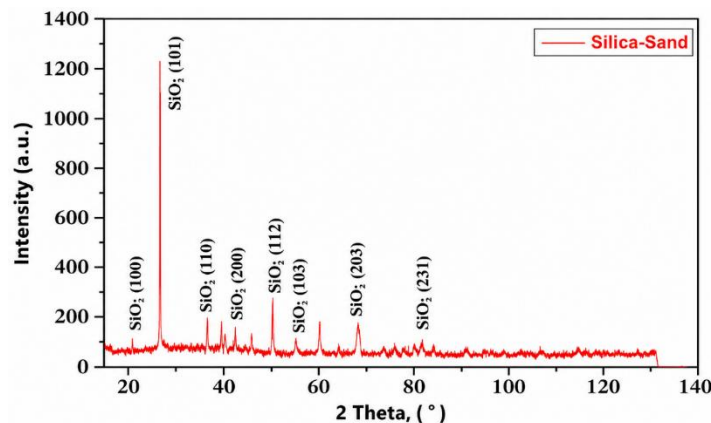


**Fig. 5.** XRD pattern obtained for 48 hours milled silica sand (MSS)

### 3.4. Chemical Composition of Tebessa Silica Sand Nanoparticles

Table 2 presents the XRF analysis results of (MNSS) nanoparticles from Tebessa (North East of

Algeria), showing Si, Al, K, Ca and Fe as the predominant elements, with their oxides  $\text{SiO}_2$ ,  $\text{Al}_2\text{O}_3$ ,  $\text{K}_2\text{O}$ ,  $\text{CaO}$  and  $\text{Fe}_2\text{O}_3$  having percentages of 97.56 wt.%, 1.37 wt.%, 0.390 wt.%, 0.285 wt.% and 0.160 wt.%, respectively.

**Table 2.** Chemical analysis data from X-ray fluorescence spectroscopy (XRF) of the Silica Sand nanoparticles

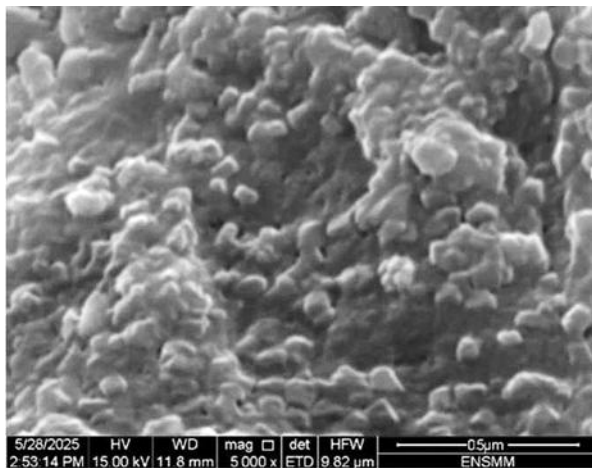
Raw material	Silica sand nanoparticles					
Elements	$\text{Al}_2\text{O}_3$	$\text{SiO}_2$	$\text{K}_2\text{O}$	$\text{CaO}$	$\text{Fe}_2\text{O}_3$	Others
Oxide (wt.%)	1.37	97.56	0.390	0.285	0.160	< 0.10%

### 3.5. Characterization of Epoxy-Silica Sand Nanocomposites

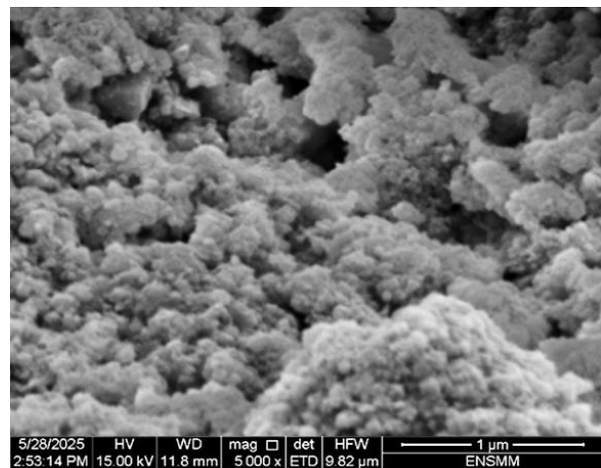
#### 3.5.1. SEM Observations and Microstructure Analysis of Epoxy/Silica Nanocomposite

In this study, a near-uniform distribution of silica sand nanoparticles was obtained within the epoxy matrix. Representative SEM images of the epoxy nanocomposites containing 42 wt.% and 62 wt.% silica, respectively (Figs. 6a and 6b), reveal the

distribution of the silica nanoparticles: (Fig. 6a) shows a uniform distribution of silica nanoparticles within the epoxy matrix for Nano Composite NC(42), while (Fig. 6b) shows a less uniform distribution for NC(62), where the silica nanoparticles are less dispersed, forming agglomerates up to 2  $\mu\text{m}$  in diameter, clearly visible at 5000 $\times$  magnification. Since the average size of the introduced particles is less than 100 nm, the  $\text{SiO}_2$  epoxy system can be defined as a nanocomposite.



a)



b)

**Fig. 6.** SEM images of the epoxy/ $\text{SiO}_2$  nanocomposites filled with: a) 42wt.% and b) 62 wt. %  $\text{SiO}_2$  nanofillers

#### 3.5.2. Development of Physical and Mechanical Properties

The study evaluated how reinforcing epoxy resin with silica sand nanoparticles affects its density and mechanical properties (tensile, flexural, and compressive strengths), with the corresponding results presented in Table 3.

Optimal mechanical properties of the epoxy-based hybrid nanocomposite were obtained by varying the constituents (epoxy, nano- $\text{SiO}_2$  reinforcement, and hardener) and averaging the responses for each independent variable, with the

best formulation given in Table 3. The formulation containing 42 wt.% silica corresponds to “the overall optimal composition” when considering compressive strength, flexural strength, microstructural homogeneity, and material economy simultaneously.

It should be noted that the optimum filler content depends on the targeted property: while 32 wt.% silica yields the maximum tensile strength, the composition containing 42 wt.% silica provides the best overall balance of compressive strength, flexural strength, microstructural quality, and material economy.

**Table 3.** Physical and mechanical properties of different (silica sand/epoxy) nanocomposites

Sample Nanocomposite NC (SiO <sub>2</sub> ) (wt. %)	Mix proportion (%)		Density (g/cm <sup>3</sup> )	Compressive strength (MPa)	Flexure strength (MPa)	Tensile strength (MPa)
	Epoxy resin (wt.%)	Nano-silica (wt.%)				
NC (00)	100%	00 %	1.153	72.185	35.432	24.362
NC (12)	88 %	12 %	1.211	89.895	37.657	26.245
NC (22)	78 %	22 %	1.266	104.525	40.752	29.572
NC (32)	68 %	32 %	1.320	109.587	44.685	33.452
NC (42)	58 %	42 %	1.376	113.685	49.723	28.375
NC (52)	48 %	52 %	1.441	110.583	43.822	21.663
NC (62)	38 %	62 %	1.514	104.758	36.275	15.245

The density values of the epoxy/silica sand nanocomposites, listed in Table 3 and plotted in Fig. 7a, increase slightly with increasing silica sand nanoparticle content from 12–62 wt.%, because silica sand is denser than neat epoxy, so its addition

as reinforcement increases the overall density of the nanocomposite. Nanocomposite samples with higher density values are therefore heavier than those with lower density values [32].

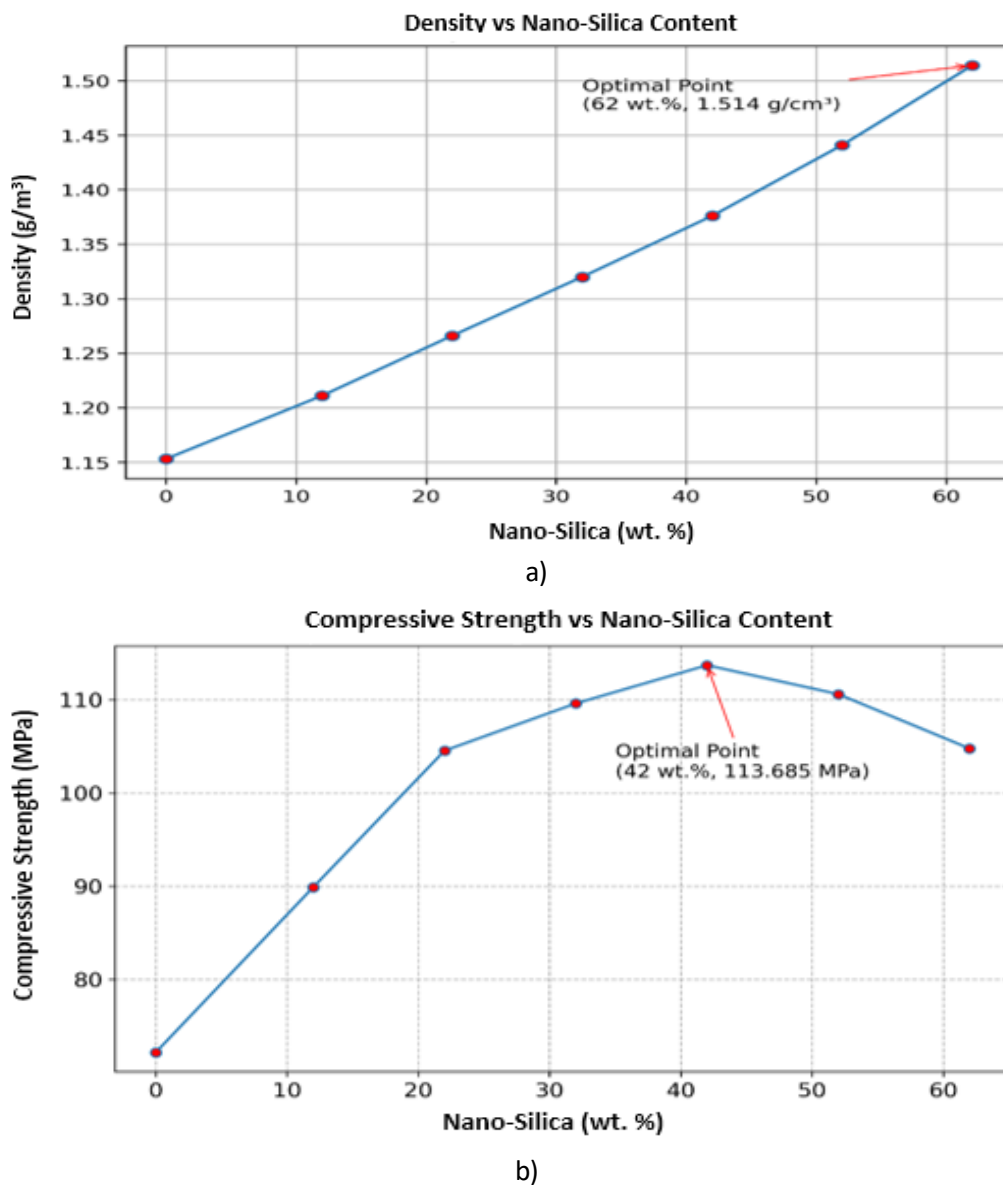


**Fig. 7.** Influence of nanosilica content (weight percentage) on: a) Density of epoxy/SiO<sub>2</sub> nanocomposites, b) Compressive strengths of epoxy/SiO<sub>2</sub> nanocomposites

The uniaxial compression test (UAC) was used to determine the compressive properties of nano-silica/epoxy-based nanocomposites (Fig. 1a), with nanosilica loadings ranging from 12 to 62 wt.%. The best mechanical test results were obtained in compression (Fig. 7b and Table 3), showing a significant, monotonically increasing improvement in compressive strength with increasing nanosilica concentration (Fig. 7b); the average strain at break increased by 57.49% over pure epoxy resin with the addition of 42 wt.% silica nanoparticles, indicating a very favorable nanofiller– matrix interaction that ensures efficient stress transfer at the interface and

results in higher strength compared to the pure epoxy.

The flexural tests (Fig. 1b) show that, as illustrated in Fig. 8a and Table 3, the average flexure values at break increase with the nano-SiO<sub>2</sub> content up to 42 wt.%. The maximum average strength at break is then 40.33% higher than that of pure epoxy resin. For nano-SiO<sub>2</sub> contents above 42 wt.%, average flexural strengths decrease (similarly to compression tests), due to particle agglomeration and the consequent reduction of matrix/load interaction.

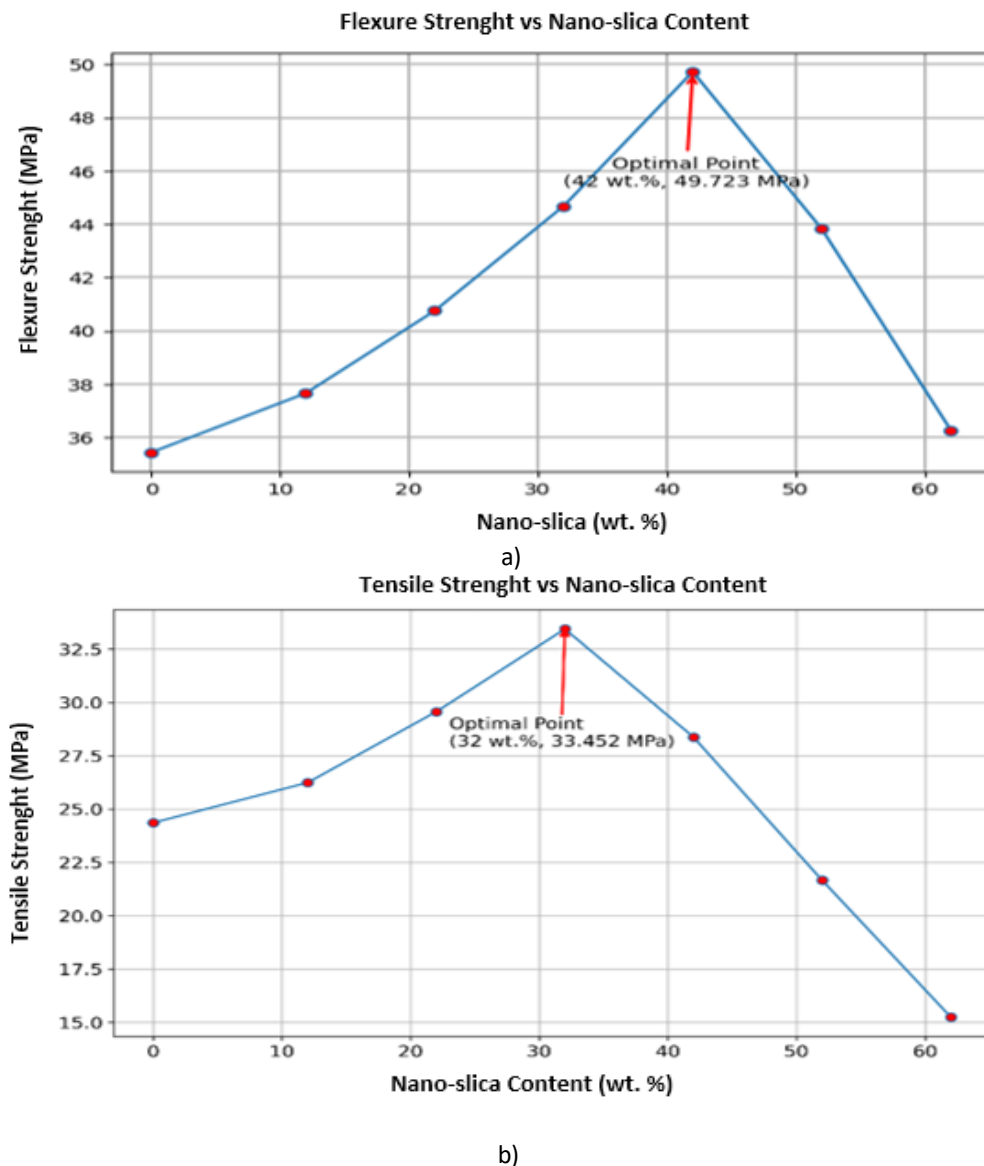


**Fig. 8.** Influence of nanosilica content (wt.%) on: a) Flexural strength of epoxy/SiO<sub>2</sub> nanocomposites, b) Tensile strength of epoxy/SiO<sub>2</sub> nanocomposites

From Table 3 and Fig. 8b, the maximum tensile strength is obtained at 32 wt.% silica content, indicating that this composition represents the optimum for tensile performance.

The average tensile strength at break is 37.31% higher than pure epoxy (reference). Adding more than 32 wt.% nano SiO<sub>2</sub> causes a decrease in compression and flexural results, due to increased

particle agglomeration and reduced matrix/filler interaction.

### 3.5.3. Fracture Surface Study

The fracture surfaces after tensile tests of neat epoxy and epoxy/SiO<sub>2</sub> nanocomposites are shown in Fig. 9. Pure epoxy (Fig. 9a) exhibits a relatively smooth, glassy, river-lined surface typical of a brittle thermosetting polymer with no large-scale plastic deformation [33]. The epoxy/silica nanocomposite with 42 wt.% SiO<sub>2</sub> (Fig. 9b) shows numerous holes (pores), cavities, and “sea wave” features, likely resulting from small molecular compounds adhering to silica nanoparticles. These

features can act as obstacles to crack propagation, causing crack deflection and energy dissipation.

Magnified images (Figs. 9c and 9d) highlight tiny crack lines, with white arrows indicating slow-propagating crack areas. The crack moves from right to left and is toughened by deflection around silica particles [34].

Cavities and pores, along with white SEM zones indicating deformation and cohesive failure where silica nanoparticles surround large parts of the polymer matrix, demonstrate that agglomeration of silica nanoparticles at higher loadings (more than 42 wt.% SiO<sub>2</sub>) contributes to the decreasing trend in mechanical properties, consistent with SEM observations such as Fig. 6b.

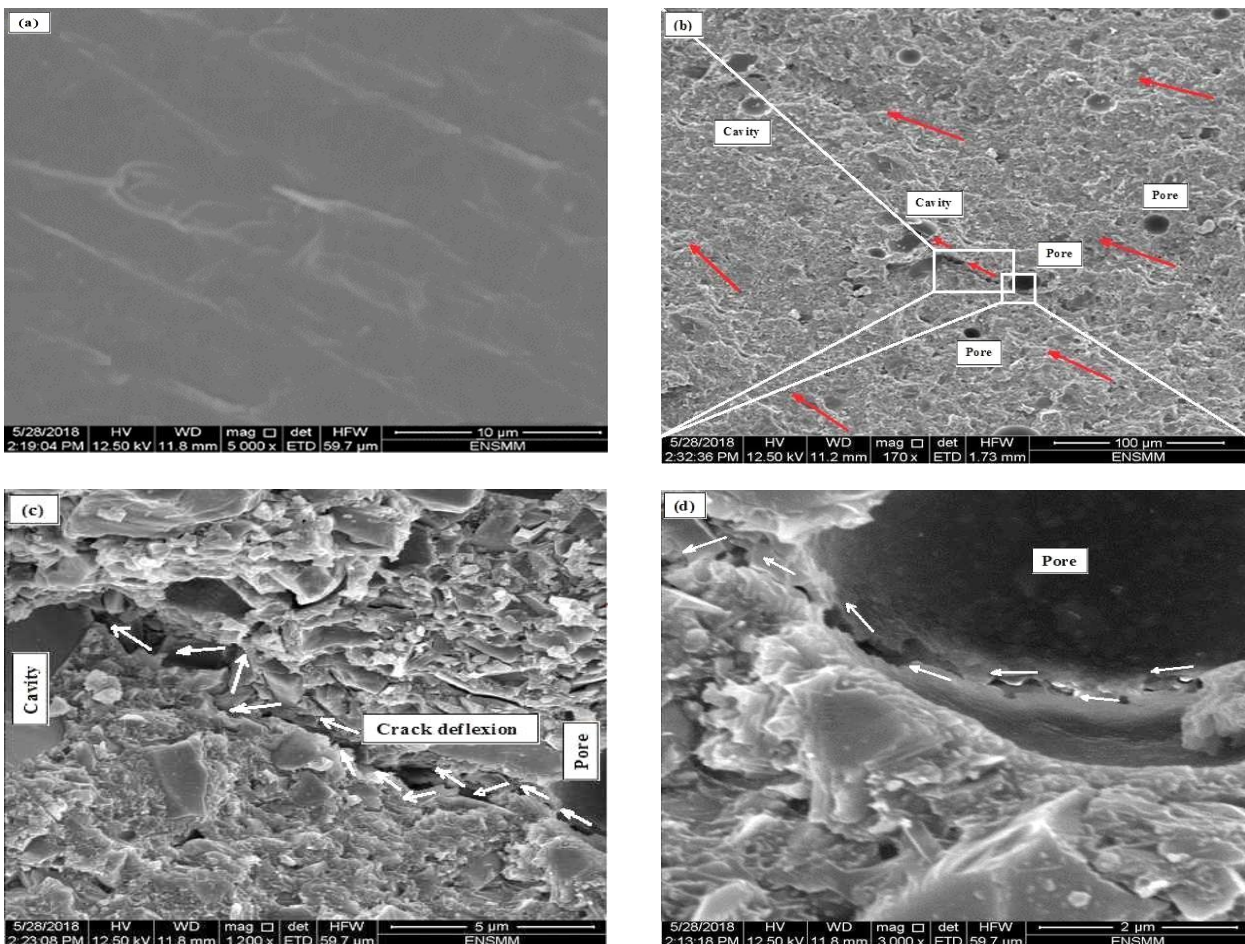


**Fig. 9.** SEM micrographs of the fracture surfaces of: a) pure epoxy (0 wt. % SiO<sub>2</sub>), b) nanocomposites (42 wt. % SiO<sub>2</sub>); (c) and (d) are magnified views of two selected areas of Fig. b), after tensile testing - crack propagation as a result of cavities and holes formed, due to improper mixture process

## 4. CONCLUSIONS

SiO<sub>2</sub> nanoparticles were successfully produced from natural silica sand by dry and ball milling, yielding high-purity SiO<sub>2</sub> (>95%) of spherical

particles (~76 nm). This route is strongly recommended from a profitability standpoint.

The mechanical (tensile, flexural, compressive), physical (density) and microstructural (morphology) properties of epoxy-based hybrid composites with nano-silica reinforcement were

optimized using a mixture design approach, showing that only nanocomposites with 42 wt.% nanofillers (58 wt.% epoxy) offer the best mechanical properties, morphology and economy.

Compared to neat epoxy, Epoxy-Resin/SiO<sub>2</sub> (ER/SiO<sub>2</sub>) nanocomposites increased ultimate compressive, flexure and tensile strengths by up to 57.49%, 40.33% and 37.31%, respectively, and SEM observations confirmed a correlation between nanocomposite morphology and mechanical properties.

#### ACKNOWLEDGEMENT

The authors warmly thank the faculty of earth sciences of Badji Mokhtar University, Annaba (Algeria) and its head, Professor Nacer Kherici, for providing the necessary financial support for this research.

#### CONFLICT OF INTEREST

The authors declare no conflict of interest.

#### REFERENCES

- [1] A. Shundo, S. Yamamoto, K. Tanaka, Network Formation and Physical Properties of Epoxy Resins for Future Practical Applications. *JACS Au*, 2(7), 2022: 1522–1542. <https://doi.org/10.1021/jacsau.2c00120>
- [2] J.J. Fekia, M. Krbata, M. Kohutiar, R. Janík, L. Kakošová, A. Breznická, M. Eckert, P. Mikuš, Comprehensive Review: Optimization of Epoxy Composites, Mechanical Properties, & Technological Trends. *Polymers*, 17(3), 2025: 271. <https://doi.org/10.3390/polym17030271>
- [3] N. Karak, Epoxy Nanocomposites with Silicon-Based Nanomaterials. *ACS Symposium Series*, 2021: 99–132. <https://doi.org/10.1021/bk-2021-1385.ch004>
- [4] J.-H. Joo, J.-R. Jeong, Y.-J. Yim, S.-H. Kim, J.-S. Bae, Recent Advances in Epoxy Resin Applications. *COJ Technical & Scientific Research*, 5(3), 2025. <https://doi.org/10.31031/COJTS.2025.05.000612>
- [5] S.S. Salins, S. Shetty, H.K. Sachidananda, Investigating energy absorption and crack propagation in natural rubber-epoxy composites: design, fabrication, and fracture analysis. *Polymer Bulletin*, 82, 2025: 5463–5491. <https://doi.org/10.1007/s00289-025-05738-y>
- [6] T.O. Ogundana, O.T. Oginni, F.A. Onuh, J. Morawo, M.O. Olagunju, Characterization of Epoxy Resin Matrix Reinforced with Silica Nanoparticles for Enhanced Mechanical Performance. *FUW Trends in Science & Technology Journal*, 9(3), 2025: 057–063.
- [7] O. Dzeikala, M. Prochoń, Silicates as fillers for polymer composites. *3<sup>rd</sup> International Scientific Conference "Chemical Technology and Engineering": Proceedings*, 21–24 June 2021, Lviv, Ukraine, pp.108–108. <https://doi.org/10.23939/cte2021.01.108>
- [8] B. Rashad, W. Bdaiwi, Exploring the role of rubber granules in modifying epoxy composites: a multi-scale approach using mechanical, thermal, and FTIR techniques. *Revista Matéria*, 29(4), 2024. <https://doi.org/10.1590/1517-7076-RMAT-2024-0702>
- [9] M. Cavasin, M. Sangermano, B. Thomson, S. Giannis, Exposure of Glass Fiber Reinforced Polymer Composites in Seawater and the Effect on Their Physical Performance. *Materials*, 12(5), 2019: 807. <https://doi.org/10.3390/ma12050807>
- [10] N. Sapiai, A. Jumahat, N. Manap, M.A. Usoff, Effect of nanofillers dispersion on mechanical properties of clay/epoxy and silica/epoxy nanocomposites. *Jurnal Teknologi*, 76(9), 2015: 107–111. <https://doi.org/10.11113/jt.v76.5687>
- [11] M.D. Kiran, H.K. Govindaraju, T. Jayaraju, N. Kumar, Review-Effect of Fillers on Mechanical Properties of Polymer Matrix Composites. *Materials Today: Proceedings*, 5(10), 2018: 22421–22424. <https://doi.org/10.1016/j.matpr.2018.06.611>
- [12] T.A. Nadzharyan, E.Y. Kramarenko, The Effect of Particle/Matrix Interface on the Local Mechanical Properties of Filled Polymer Composites: Simulations and Theoretical Analysis. *Polymers*, 17(1), 2025: 111. <https://doi.org/10.3390/polym17010111>
- [13] F. Rothenhäusler, M. Kettenbach, H. Ruckdaeschel, Influence of the Stoichiometric Ratio on the Curing Kinetics and Mechanical Properties of Epoxy Resin Cured with a Rosin-Based Anhydride. *Macromolecular Materials and Engineering*, 308(11), 2023: 2300122. <https://doi.org/10.1002/mame.202300122>
- [14] D. Shen, X. Pi, L. Cai, X. Wang, C. Wu, R. Liu, Investigation of Adsorption and Young's Modulus of Epoxy Resin-Sand Interfaces Using

- Molecular Dynamics Simulation. *Applied Sciences*, 14(22), 2024: 10383.  
<https://doi.org/10.3390/app142210383>
- [15] W.A. Ali, S.E. Richards, R.H. Alzard, Unlocking the potential of ball milling for nanomaterial synthesis: An overview. *Journal of Industrial and Engineering Chemistry*, 149, 2025: 63-93.  
<https://doi.org/10.1016/j.jiec.2025.01.054>
- [16] T. Kim, J. Lee, Silicon nanoparticles: fabrication, characterization, application and perspectives. *Micro and Nano Systems Letters*, 11, 2023: 18.  
<https://doi.org/10.1186/s40486-023-00184-9>
- [17] C. Vanhoof, J.R. Bacon, U.E.A. Fittschen, L. Vincze, Atomic spectrometry update: a review of advances in X-ray fluorescence spectrometry and its special applications. *Journal of Analytical Atomic Spectrometry*, 36(9), 2021: 1797–1812.  
<https://doi.org/10.1039/D1JA90033A>
- [18] J.D. Russell, M.S. Madhukar, M.S. Genidy, A.Y. Lee, A New Method to Reduce Cure-Induced Stresses in Thermoset Polymer Composites, Part III: Correlating Stress History to Viscosity, Degree of Cure, and Cure Shrinkage. *Journal of Composite Materials*, 34(22), 2000: 1926-1947.  
<https://doi.org/10.1106/UY9U-F2QW-2FKK-91KG>
- [19] J. Rybica, T. Purse, B. Parlour, A Generic Cost Estimating Approach for a Composite Manufacturing Process Assessment. *Advances in Transdisciplinary Engineering*, 2021: 414-418. <https://doi.org/10.3233/ATDE210071>
- [20] G.V. Kozlov, I.V. Doblin, Transfer of mechanical stress from polymer matrix to nanofiller in dispersion-filled nanocomposites. *Inorganic Materials: Applied Research*, 10(1), 2019: 226–230.  
<https://doi.org/10.1134/S2075113319010167>
- [21] H.E.M. Sallam, U.A. Khashaba, M. Abd-Elhamid, A.A. Megahed, M.A. Megahed, Ultrasonic mixing of nanoparticles in epoxy resin. In: *Proceedings of the 1<sup>st</sup> International Conference on Nano-Technology for Green and Sustainable Construction*, 13-15 March 2010, Cairo, Egypt, pp.312-316.
- [22] A.T. Bhatt, P.P. Gohil, V. Chaudhary, Degassing and layers variation effect on composite processing by vacuum assisted resin transfer moulding. *Journal of Engineering Research*, 10(2), 2022: 184-192.  
<https://doi.org/10.36909/jer.9941>
- [23] S. Rangrej, V. Mehta, V. Ayar, M. Sutaria, Effects of stir casting process parameters on dispersion of reinforcement particles during preparation of metal composites. *Materials Today: Proceedings*, 43, 2021, 471-475.  
<https://doi.org/10.1016/j.matpr.2020.11.1002>
- [24] V. Obradović, D. Simic, P. Sejkot, M. Vokáč, Moisture absorption characteristics and effects on mechanical properties of Kolon/epoxy composites. *Current Applied Physics*, 26(1), 2021: 16-23.  
<https://doi.org/10.1016/j.cap.2021.03.015>
- [25] J.R. Grogan, A.L. Nicuşan, C.R.K. Windows-Yule, Effect of cylinder wall parameters on the final packing density of mono-disperse spheres subject to three-dimensional vibrations. *Particuology*, 91, 2024: 211-225.  
<https://doi.org/10.1016/j.partic.2024.01.017>
- [26] J.S. Giunta, Flow Patterns of Granular Materials in Flat-Bottom Bins. *Journal of Engineering for Industry, Transactions of the ASME*, 91(2), 1969: 406-413.  
<https://doi.org/10.1115/1.3591585>
- [27] I. Miturska, A. Rudawska, M. Müller, M. Hromasová, The influence of mixing methods of epoxy composition ingredients on selected mechanical properties of modified epoxy construction materials. *Materials*, 14(2), 2021: 411. <https://doi.org/10.3390/ma14020411>
- [28] ASTM D792-20, Standard test methods for density and specific gravity (relative density) of plastics by displacement. *ASTM International*, West Conshohocken, PA, USA, 2020.  
<https://doi.org/10.1520/D0792-20>
- [29] ASTM C349-97, Standard Test Method for Compressive Strength of Hydraulic-Cement Mortars (Using Portions of Prisms Broken in Flexure). *ASTM International*, West Conshohocken, PA, USA, 1997.  
<https://doi.org/10.1520/C0349-97>
- [30] A.P. Wemhoff, A.J. Webb, Investigation of nanoparticle agglomeration on the effective thermal conductivity of a composite material. *International Journal of Heat and Mass Transfer*, 97, 2016: 432-438.  
<https://doi.org/10.1016/j.ijheatmasstransfer.2016.02.027>
- [31] A. Ali, Y.W. Chiang, R.M. Santos, X-ray Diffraction Techniques for Mineral Characterization: A Review for Engineers of the Fundamentals, Applications, and Research Directions. *Minerals*, 12(2), 2022: 205.  
<https://doi.org/10.3390/min12020205>
- [32] R. Babba, K. Hebbache, A. Douadi, M. Boutlikht, R. Hammouche, S. Dahmani, G. Del Serrone, L. Moretti, Impact of Silica Sand on Mechanical Properties of Epoxy Resin Composites and

- Their Application in CFRP– Concrete Bonding. *Applied Sciences*, 14(15), 2024: 6599.  
<https://doi.org/10.3390/app14156599>
- [33] R. Zhao, W. Luo, Fracture surface analysis on nano-SiO<sub>2</sub>/epoxy composite. *Materials Science and Engineering: A*, 483–484, 2008: 313-315.  
<https://doi.org/10.1016/j.msea.2006.08.151>
- [34] F.J. Guild, A.J. Kinloch, K. Masania, S. Sprenger, A.C. Taylor, The fracture of thermosetting epoxy polymers containing silica nanoparticles. *Strength, Fracture and Complexity*, 11(2–3), 2018: 137–148.  
<https://doi.org/10.3233/SFC-180219>